ACCOUNTS
of chemical research

The Structural Chemistry of Metallocorroles: Combined X-ray Crystallography and Quantum Chemistry Studies Afford Unique Insights

KOLLE E. THOMAS,[†] ABRAHAM B. ALEMAYEHU,[†] JEANET CONRADIE,[†,‡] CHRISTINE M. BEAVERS,[§] AND ABHIK GHOSH*,[†]

[†]*Department of Chemistry and Center for Theoretical and Experimental Chemistry, University of Tromsø, 9037 Tromsø, Norway,* [‡]*Department of Chemistry, University of the Free State, 9300 Bloemfontein, Republic of South Africa, and* [§]*Advanced Light Source, Lawrence Berkeley National Laboratory, Berkeley, California 94720-8229, United States*

RECEIVED ON NOVEMBER 12, 2011

CONSPECTUS

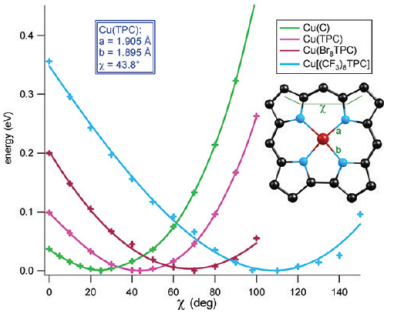

Although they share some superficial structural similarities with porphyrins, corroles, trianionic ligands with contracted cores, give rise to fundamentally different transition metal complexes in comparison with the dianionic porphyrins. Many metallocorroles are formally high-valent, although a good fraction of them are also noninnocent, with significant corrole radical character. These electronic-structural characteristics result in a variety of fascinating spectroscopic behavior, including highly characteristic, paramagnetically shifted NMR spectra and textbook cases of charge-transfer spectra. Although our early research on corroles focused on spectroscopy, we soon learned that the geometric structures of metallocorroles provide a fascinating window into their electronic-structural characteristics. Thus, we used X-ray structure determinations and quantum chemical studies, chiefly using DFT, to obtain a comprehensive understanding of metallocorrole geometric and electronic structures.

This Account describes our studies of the structural chemistry of metallocorroles. At first blush, the planar or mildly domed structure of metallocorroles might appear somewhat uninteresting particularly when compared to metalloporphyrins. Metalloporphyrins, especially sterically hindered ones, are routinely ruffled or saddled, but the missing *meso* carbon apparently makes the corrole skeleton much more resistant to nonplanar distortions. Ruffling, where the pyrrole rings are alternately twisted about the M–N bonds, is energetically impossible for metallocorroles. Saddling is also uncommon; thus, a number of sterically hindered, fully substituted metallocorroles exhibit almost perfectly planar macrocycle cores.

Against this backdrop, copper corroles stand out as an important exception. As a result of an energetically favorable Cu(d_{x2-y2})–corrole(π) orbital interaction, copper corroles, even sterically unhindered ones, are inherently saddled. Sterically hindered substituents accentuate this effect, sometimes dramatically. Thus, a crystal structure of a copper β-octakis-(trifluoromethyl)-*meso*-triarylcorrole complex exhibits nearly orthogonal, adjacent pyrrole rings. Intriguingly, the formally isoelectronic silver and gold corroles are much less saddled than their copper congeners because the high orbital energy of the valence d_{x2-y2} orbital discourages overlap with the corrole π orbital. A crystal structure of a gold β-octakis-(trifluoromethyl)-*meso*-triarylcorrole complex exhibits a perfectly planar corrole core, which translates to a difference of 85° in the saddling dihedral angles between analogous copper and gold complexes. Gratifyingly, electrochemical, spectroscopic, and quantum chemical studies provide a coherent, theoretical underpinning for these fascinating structural phenomena.

With the development of facile one-pot syntheses of corrole macrocycles in the last 10–15 years, corroles are now almost as readily accessible as porphyrins. Like porphyrins, corroles are promising building blocks for supramolecular constructs such as liquid crystals and metal–organic frameworks. However, because of their symmetry properties, corrole-based supramolecular constructs will probably differ substantially from porphyrin-based ones. We are particularly interested in exploiting the inherently saddled, chiral architectures of copper corroles to create novel oriented materials such as chiral liquid crystals. We trust that the fundamental structural principles uncovered in this Account will prove useful as we explore these fascinating avenues.

Published on the Web 03/23/2012 www.pubs.acs.org/accounts
10.1021/ar200292d

1. Introduction

Porphyrin chemistry, nicely summarized in a single volume just over 35 years ago,[1] is today a veritable ocean of knowledge. Even porphyrin analogues, such as carbaporphyrins, heteroporphyrins, and expanded and contracted porphyrins, mere curiosities a couple of decades ago, need book-length treatment for adequate coverage.[2] The sheer diversity of such ligands is breathtaking, and any attempt to enumerate them is certain to be out-of-date within a few months. A variety of considerations drives this enterprise, including synthesis for synthesis' sake, creating molecules with novel geometric and electronic structures, of which Möbius aromatics are a spectacular example,[3] and technological and biomedical applications. Of particular interest from the point of view of applications are ligands that can be accessed with reasonable ease by moderately skilled synthetic chemists, in reasonable quantities (hundreds of milligrams) and within reasonable time frames (in under about a week). A number of porphyrinoids fulfill this criterion, and corroles are preeminent among them.[4]

Although corroles cannot match the biological importance of porphyrins, corrole chemistry has begun to rival porphyrin chemistry in other respects, particularly in terms of the rich coordination chemistry and the wide range of applications. The remarkable growth of the corrole field is a relatively recent occurrence, having begun with reports of one-pot syntheses of corroles only some 15 years ago.[5,6] Many fundamental aspects of corroles are therefore still being discovered. Indeed, important aspects such as structural chemistry, spectroscopy, and quantum chemical studies of corrole derivatives remain to be reviewed; these are actually the areas where we have focused our attention over the past decade or so and where we hope to continue to contribute. Over a hundred crystal structures of corrole derivatives have now been reported, allowing for structural trends to be discerned and generalizations made; these form the subject of this Account.

Much of this work was conducted at the University of Tromsø by authors K.E.T. and A.B.A. and has focused on coinage metal corroles. To the extent it makes sense to talk about an overarching goal, we were motivated by a desire to discover unusual geometric and electronic structures, particularly nonplanar and noninnocent systems, a point of view that proved rewarding. Our findings have allowed us to formulate generalizations and rules of thumb governing the structural chemistry of metallocorroles, as discussed below. While X-ray crystallography was the main workhorse

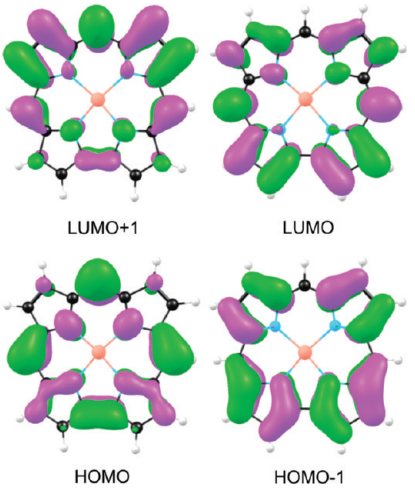

FIGURE 1. Gouterman four orbitals: the two HOMOs and the two LUMOs of $[Mg(C)]^-$.

in this effort, quantum chemical calculations, mostly using density functional theory (DFT), proved invaluable in placing the geometric structures in an appropriate electronic-structural context. The close synergy between experimental and DFT studies is perhaps the most distinctive aspect of this work. The theoretical work was initiated by former postdoctoral associate Emmanuel Gonzalez and subsequently expanded upon by author J.C.

As tetrapyrrolic, aromatic N_4 ligands, corroles are superficially similar to porphyrins. A key similarity involves Gouterman's four-orbital model for porphyrins, according to which the two HOMOs are near-degenerate, and so are the two LUMOs, and these four frontier MOs are well separated energetically from all other occupied and unoccupied MOs.[7] The rule applies to free base porphyrins and complexes involving closed-shell ions and our early quantum chemical studies showed that the model applied to corroles as well.[8] These four MOs are depicted for an idealized C_{2v} metallocorrole, $[Mg(C)]^-$, in Figure 1. Analogous porphyrins and corroles thus exhibit roughly similar electronic absorption spectra and photophysical properties. Beyond that, however, the similarities rapidly give way to a plethora of moderate and major differences.

A key difference obviously centers around the fact the corroles are trianionic ligands, whereas porphyrins are dianionic. Thus, for a given metal, overall stoichiometries are often different between related metalloporphyrins and metallocorroles. The trianionic corroles are also much more effective than porphyrins at stabilizing high-valent transition metal centers such as $Cr^{V}O$, Mn^{IV}–Ar, Fe^{IV}–Ar, Fe^{IV}–O-Fe^{IV}, and Ag^{III}, although in some cases such as

Cu and FeCl,[9] a noninnocent corrole$^{\bullet 2-}$ formulation has been preferred.

Table 1 presents a list of mononuclear metallocorrole crystal structures reported to date, multinuclear complexes having been omitted for simplicity. Abbreviations for various ligands are listed in Table 2 and are used in the text without further explanation. One of the more general features of metallocorrole structures is the shortness of the metal−nitrogen (M−N) distances, which are typically about 1.9 Å for first-row transition ions, compared to a value of 2.0 Å or higher for metalloporphyrins. This may be seen from Table 1 for Cr, Mn, Fe, and Co corroles as well as for Al, Ga, and Ge complexes. For second- and third-row transition ions, the M−N distances are somewhat longer, 1.95−2.00 Å, as is the case for Mo, Ru, Rh, Ag, Re, Ir, and Au corroles, as well as for Sb and Sn corroles.

Aside from M−N distances, the structural chemistry of metallocorroles differs from that of metalloporphyrins in numerous other ways. Some of these differences are rather unexpected and these form the heart of this Account.

2. The Planar Conformation

Metallocorroles are generally planar, a generalization that should be clear from a perusal of Table 1. It would be wrong, however, to construe this generalization as a suggestion that the structural chemistry of corroles is "uninteresting" or "boring". Seen from a porphyrin perspective, the planarity of some of the more sterically hindered metallocorrole frameworks is remarkable. Thus, the undecasubstituted Co corroles Co[Et_8TPC](PPh_3) (WETBUS)[10] and the related Ir corrole Ir[Br_8TPFPC](NMe_3)$_2$ (COHYOO)[11] are characterized by planar corrole macrocycles (Figure 2). Analogous dodecasubstituted porphyrins, regardless of the coordinated central ion, by contrast, are invariably strongly saddled.

To appreciate these structures in terms of an energetics picture, we evaluated DFT saddling potentials for a set of four Co-PPh_3 corroles, involving progressively sterically hindered ligands: unsubstituted corrole (C), *meso*-triphenylcorrole (TPC), β-octabromo-*meso*-triphenylcorrole (Br_8TPC), and β-octakis(trifluoromethyl)-*meso*-triphenylcorrole [$(CF_3)_8$TPC].[12] As shown in Figure 3, planar conformations were indicated for all four complexes, which is broadly consistent with experimental observations but is nonetheless remarkable. In the absence of special electronic effects, peripheral substituents, however sterically hindered, are not particularly effective at engendering saddling in metallocorroles.

3. The Domed Conformation

An interesting aspect of metallocorroles compared with metalloporphyrins is a preponderance of five-coordinate structures, concomitant with a relative rarity of six-coordinate ones.[4] It is thus understandable that domed conformations are not uncommon for metallocorroles. True macrocycle doming, however, is more uncommon than cases where the coordinated metal simply sits atop a relatively planar corrole. As in the case of porphyrins, true doming is associated with large coordinated atoms such as Mo, Re, Sn, and Bi that would not fit well within a planar macrocycle. A selection of domed metallocorrole crystal structures is shown in Figure 4.[13]

4. Ruffling, a Forbidden Distortion Mode

Table 1 lists a handful of saddled metallocorroles, chiefly involving copper, but note the striking absence of the ruffled conformation. By contrast, ruffling is one of the most common distortion modes for porphyrins, where it is most frequently associated with a small central metal ion such as Ni(II) or low-spin Fe(III), but is also known to result from sterically hindered *meso*-substituents such as perfluoroalkyl and *t*-butyl. The following examples illustrate well this key difference between porphyrins and corroles.

Coordination of very small ions such as phosphorus(V), which has an ionic radius of only 0.52 Å, invariably leads to strong ruffling in porphyrins.[14] By contrast, the sole structurally characterized P^V corrole [P(Et_2Me_6C)(OH)]$^+$ (NUHDUP)[15] has a planar macrocycle.

To compare the effects of *meso*-CF_3 groups on corroles versus porphyrins, we determined single-crystal X-ray structures of Co^{III}[$(CF_3)_3$Cor](PPh_3) [$(CF_3)_3$Cor = *meso*-tris(trifluoromethyl)corrolato] (UWULEE)[12] and Cu[$(CF_3)_4$Por] [$(CF_3)_4$Por = *meso*-tetrakis(trifluoromethyl)porphyrinato] (ITEXUB).[16] As shown in Figure 5, the corrole is planar and the porphyrin strongly ruffled. These results are consistent with the X-ray structures of Re[$(CF_3)_3$Cor](O) (NUHJOP)[17] and Ga[(*n*-$C_3F_7)_3$Cor](py) (py = pyridine, QORBOO),[18] which also exhibit planar corrole ligands. In contrast, the *meso*-perfluoroalkylated metalloporphyrins Zn[(*n*-$C_3F_7)_4$Por](py) (TOJLIN)[19] and Ni[(*n*-$C_3F_7)_4$Por] (HUPDEB)[20] exhibit strongly ruffled macrocycles.

Again, to place these observations in an energetics context, we evaluated BP86-D ruffling and saddling potentials (Figure 6) for selected cobalt and copper porphyrins and corroles. Figure 6a defines the ruffling and saddling dihedrals. Figure 6b confirms planar minima for all cobalt

TABLE 1. Select Experimental Structural Parameters (Å, °) for Mononuclear Metallocorroles[a]

no.	Z	complex	M	M−N_1/N_2[a]	M−N_3/N_4[a]	M−N_4	L		M−L		conformation	χ[b]	CSD[c]
1	13	Al[TPFPC](Py$_2$)	Al	1.896	1.891	0.003	Py	Py	2.201	2.215	planar		NILPUU
2	13	Al[I$_4$TPFPC](Py)$_2$	Al	1.887	1.911	0.007	Py	Py	2.173	2.179	flat	–	HAFQEM
3	15	P[Et$_2$Me$_6$C](OH)	P	1.815	1.796	0.407	OH	–	1.537	–	planar		NUHDUP
4	24	Cr[TPFPC](NMes)	Cr	1.948	1.938	0.537	Mes	–	2.991	–	planar		NAQDAL
5	24	Cr[TPFPC](N-pTos)	Cr	1.954	1.931	0.569	NpTos	–	1.653	–	planar		SEVXEX
6	24	Cr[TPFPC](O)	Cr	1.939	1.932	0.562	O	–	1.570	–	saddled	17.1	WIZRUS
7	24	Cr[(BT-PFP-pBrPC](O)	Cr	1.941	1.921	0.572	O	–	1.57	–	planar		XOZXIU
8	24	Cr[TPFPC](Py$_2$)	Cr	1.947	1.928	0.002	Py	Py	2.109	2.129	planar		YIDZEQ
9	25	Mn[Et$_6$Me$_2$C](Ph)	Mn	1.902	1.881	0.285	Ph	–	2.019	–	planar		CISGUH
10	25	Mn[Et$_6$Me$_2$C](4BrPh)	Mn	1.900	1.897	0.247	BrC$_6$H$_4$		2.019	–	planar		CISHAO
11	25	Mn[TMePyC](H$_2$O)$_2$	Mn	1.912	1.894	0.000	H$_2$O	H$_2$O	2.328	2.328	planar		FAFXER
12	25	Mn[Et$_8$T$_2$C](I)	Mn	1.938	1.918	0.361	I	–	2.633	–	planar		GIFJEL
13	25	Mn[TPFPC](NMes)	Mn	1.931	1.901	0.513	NMes	–	2.976	–	domed		OGOJID
14	25	Mn[Et$_6$Me$_2$C]	Mn	1.901	1.887	0.011	–	–	–	–	planar		ROCFAQ
15	25	Mn[TPFPC](EtAc)	Mn	1.915	1.907	0.216	OC(CH$_3$)OEt	–	2.172	–	planar		SEVXAT
16	25	Mn[Et$_4$R$_2$Me$_2$C](Cl)	Mn	1.942	1.918	0.407	Cl	–	2.338	–	planar		TORMET
17	25	Mn[BMePyPFPC](OHMe)	Mn	1.918	1.905	0.209	OHCH$_3$	–	2.194	–	planar		WIDQUW
18	25	Mn[TPFPC](OPPh$_3$)	Mn	1.921	1.912	0.288	OPPh$_3$	–	2.075	–	planar		XARTIT
19	25	Mn[Et$_8$Ph$_2$C](I)	Mn	1.945	1.922	0.380	I	–	2.663	–	planar		XIDRUY
20	25	Mn[TPFPC](Br)	Mn	1.936	1.915	0.416	Br	–	2.428	–	planar		YAWQAO
21	25	Mn[TPFPC](Cl)	Mn	1.940	1.924	0.427	Cl	–	2.312	–	slightly domed		YAWQES
22	26	Fe[TPFPC](Py$_2$)	Fe	1.905	1.870	0.015	Py	Py	2.022	2.042	planar		AGUKUI
23	26	Fe[TPFPC](NO)	Fe	1.924	1.897	0.465	NO	–	2.812	–	planar		AGULAP
24	26	Fe[TDCPC](NO)	Fe	1.920	1.900	0.452	NO	–	2.803	–	planar		AGULET
25	26	Fe[Me$_8$TPC](Cl)	Fe	1.922	1.893	0.386	Cl	–	2.242	–	slightly saddled	12.0	CAYCAH
26	26	Fe[Et$_8$AcC](Cl)	Fe	1.894	1.870	0.399	Cl	–	2.264	–	planar		DOPBOA
27	26	Fe[DpivNP-TOMeP-C](NO)	Fe	1.943	1.909	0.522	NO		1.65		planar		DOXBAU
28	26	Fe[TPFPC](Cl)	Fe	1.920	1.882	0.367	Cl	–	2.238	–	planar		MELBOU
29	26	Fe[TPFPC](Py$_2$)	Fe	1.917	1.866	0.001	Py	Py	2.028	2.032	planar		QONXOG
30	26	Fe[OEC](Cl)	Fe	1.923	1.890	0.422	Cl	–	2.254	–	planar		SUMWUS
31	26	Fe[OEC](Ph)	Fe	1.885	1.858	0.272	Ph	–	1.984	–	planar		SUMXED
32	26	Fe[OEC](Py)	Fe	1.911	1.875	0.273	Py	–	2.188	–	planar		SUMXIH
33	26	Fe[TTC](NO)	Fe	1.929	1.898	0.455	NO	–	2.806	–	planar		VEGFET
34	26	Fe[TpOMePC](NO)	Fe	1.911	1.884	0.449	NO	–	1.702	–	planar		VEGFIX
35	26	Fe[OEC](Ph)	Fe(IV)	1.877	1.900	0.242	Ph	–	1.966	–	planar		ZOKCIL
36	26	Fe[TMesC](Cl)	Fe	1.924	1.896	0.421	Cl	–	2.23	–	domed		ATIXEH
37	27	Co[TCF$_3$C](PPh$_3$)	Co	1.885	1.874	0.269	PPh$_3$		2.203		planar		UWULEE
38	27	Co[TPFPC](PPh$_3$]	Co	1.886	1.872	0.262	PPh$_3$	–	2.205	–	planar		BAQPUF
39	27	Co[T2ThC](Py$_2$)	Co	1.896	1.862	0.015	Py	Py	1.981	2.004	planar		GEDQEM
40	27	Co[T3ThC](Py$_2$)	Co	1.899	1.869	0.007	Py	Py	1.998	1.998	planar		GEDQIQ
41	27	Co[(CF$_3$)$_2$PFC](PPh$_3$)	Co	1.887	1.871	0.268	PPh$_3$	–	2.215	–	planar		GIBXUL
42	27	Co[TPC](PPh$_3$)	Co	1.889	1.866	0.280	PPh$_3$	–	2.201	–	planar		KIMQOM
43	27	Co[Ps$_2$TPFPC](PPh$_3$)	Co	1.877	1.871	0.266	PPh$_3$	–	2.225	–	planar		MEWMIK
44	27	Co[Ps$_2$TPFPC'](PPh$_3$)	Co	1.861	1.855	0.264	PPh$_3$	–	2.217	–	planar		MOLGOJ
45	27	Co[Br$_8$TNPC](PPh$_3$)	Co	1.917	1.869	0.300	PPh$_3$	–	2.207	–	saddled	51.1	QIQCUO
46	27	Co[Me$_4$Ph$_5$C](Py$_2$)	Co	1.903	1.885	0.021	Py	Py	1.981	2.002	planar		QUQMAQ
47	27	Co[TPFPC](Py$_2$)	Co	1.900	1.878	0.002	Py	Py	1.994	1.995	planar		TIJBAP
48	27	Co[OEC](Ph)	Co	1.868	1.844	0.185	Ph	–	1.937	–	planar		TOPKAK
49	27	{Co[OEC](Ph)}$^+$	Co	1.866	1.834	0.165	Ph	–	1.969	–	planar		TOPKEO
50	27	Co[Et$_8$TPC](PPh$_3$)	Co	1.898	1.879	0.281	PPh$_3$	–	2.206	–	saddled	6.3	WETBUS
51	27	Co[TPFPC](Cl)	Co	1.917	1.887	0.413	Cl	–	2.24	–	saddled		UWOBUE
52	28	Ni[Et$_4$Me$_4$C]	Ni	1.859	1.833	0.008	–	–	–	–	planar		RINBUL
53	29	Cu[(CF$_3$)$_8$TpFPC]	Cu	1.925	1.922	0.013					saddled	84.5	OVEVAN
54	29	Cu[TDCPC]	Cu	1.882	1.883	0.014	–	–	–	–	saddled	32.8	BERVOK
55	29	Cu[T2ThC]	Cu	1.889	1.889	0.026	–	–	–	–	saddled	49.6	GEDQAI
56	29	Cu[TPC]	Cu	1.892	1.894	0.031	–	–	–	–	saddled	46.0	KAGGIJ

TABLE 1. Continued

no.	Z	complex	M	M−N_1/N_2[a]	M−N_3/N_4[a]	M−N_4	L		M−L		conformation	χ[b]	CSD[c]
57	29	Cu[$Et_4Me_2R_2C$]	Cu	1.896	1.885	0.017	–	–	–	–	saddled	32.0	LADJUX
58	29	Cu[DP*p*OMePC]	Cu	1.908	1.896	0.034	–	–	–	–	saddled	42.2	LUMDON
59	29	Cu[(pCF_3P)$_2$*p*OMePC]	Cu	1.902	1.890	0.001	–	–	–	–	saddled	46.2	LUMDUT
60	29	Cu[TCbPC]	Cu	1.863	1.884	0.053	–	–	–	–	saddled	36.1	QAQVOU
61	29	Cu[Et_8Ph_2C]	Cu	1.900	1.894	0.017	–	–	–	–	saddled	21.1	QEVQAK
62	29	Cu[Et_4Me_4C]	Cu	1.884	1.874	0.027	–	–	–	–	saddled	14.4	RINCAS
63	29	Cu[Dmes-Py*C]	Cu	1.891	1.881	0.005	–	–	–	–	saddled	28.0	TURYUB
64	29	Cu[Br_8(*p*OMeP)$_2$TC]	Cu	1.913	1.916	0.016	–	–	–	–	saddled	67.8	UKETAG
65	29	Cu[DPFPThC]	Cu	1.901	1.881	0.021	–	–	–	–	saddled	42.9	VAJMEA
66	29	Cu[TNPC]	Cu	1.872	1.867	0.002	–	–	–	–	saddled	32.5	IROGAY
67	29	Cu[(*o*-TolPh)(PFP)$_2$C](Cl)	Cu	1.905	1.891	0.011	–	–	–	–	saddled	40.2	ASUYET
68	29	Cu[TPTBuC]	Cu	1.912	1.906	0.021	–	–	–	–	saddled	51.4	CAHYIV
69	29	Cu[TPTBzC]	Cu	1.920	1.931	0.022	–	–	–	–	saddled	15.4	CAHYOB
70	31	Ga[TPFPC−COOH](Py)	Ga	1.946	1.959	0.402	Py	–	2.024	–	slightly domed		BAWHIR
71	31	Ga[NO_2-TPFPC](Py)	Ga	1.934	1.956	0.376	Py	–	2.039	–	slightly domed		MOLGAV
72	31	Ga[DNO_2-TPFPC](Py_2)	Ga	1.911	1.933	0.053	Py	Py	2.233	2.284	planar		MOLGEZ
73	31	Ga[TNO_2-TPFPC](Py)	Ga	1.914	1.956	0.301	Py	–	2.055	–	slightly domed		MOLGID
74	31	Ga[TPFPC](Py)	Ga	1.941	1.941	0.411	Py	–	2.037	–	planar		QATMUT
75	31	Ga[TC_3F_7C](Py)	Ga	1.923	1.940	0.312	Py	–	2.073	–	planar		QORBOO
76	31	Ga[TPFPC−CHO](Py)	Ga	1.931	1.937	0.391	N	–	2.05	–	slightly domed		UGIRUY
77	32	Ge[Br_6TPC](OHMe)	Ge	1.911	1.934	0.446	$OHCH_3$	–	1.765	–	planar		WIDFEV
78	32	Ge[TPFPC](Me)	Ge	1.939	1.931	0.539	CH_3	–	1.923	–	domed	–	HAFYIY
79	32	Ge[TPFPC](OEt)	Ge	1.938	1.924	0.474	OEt	–	1.789	–	domed	–	HAFYOE
80	32	Ge[TPFPC]-(CH_2CH_2COOMe)	Ge	1.937	1.930	0.533	$CH_2CH_2COOCH_3$	–	1.928	–	domed	–	HAFYUK
81	42	Mo[TPFPC](O)	Mo	2.039	2.034	0.729	O	–	1.684	–	domed		YEBTIJ
82	44	Ru[TPFPC](NO)	Ru	1.993	1.963	0.535	NO	–	2.884	–	slightly domed		HUQJEI
83	45	Rh[TPFPC](Py)(PPh_3)	Rh	1.965	1.955	0.096	Py	PPh_3	2.212	2.297	planar		DABXUA
84	45	Rh[TDCPC](Py)(PPh_3)	Rh	1.973	1.953	0.108	Py	PPh_3	2.185	2.314	planar		DABYAH
85	45	Rh[TPFPC]($Py)_2$	Rh	1.968	1.940	0.015	Py	Py	2.060	2.065	planar		DADJUO
86	45	Rh[TPFPC](H_2O)(Py*)	Rh	1.993	1.963	0.111	H_2O	$NC_{12}H_{15}$	2.048	2.151	planar		DADKAV
87	45	Rh[Me_8C]($AsPh_3$)	Rh	1.958	1.931	0.257	$AsPh_3$	–	2.311	–	planar		KEKKOA
88	45	Rh[TPFPC](PPh_3)	Rh	1.972	1.770	0.277	PPh_3	–	2.222	–	slightly domed		MELBUA
89	45	Rh[TPFPC]($MePy)_2$	Rh	1.959	1.942	0.001	NC_6H_7	NC_6H_7	2.036	2.042	planar		TANGIZ
90	47	Ag[TTC]	Ag	1.960	1.948	0.003	–	–	–	–	saddled	40.2	GUWXOL
91	47	Ag[TNO_2-$Et_4R_2Me_2C'$]	Ag	1.975	1.950	0.006	–	–	–	–	saddled	16.7	JIWCIC
92	50	Sn[OEC](Ph)	Sn	2.066	2.068	0.721	Ph	–	2.106	–	domed		FEGDAW
93	50	Sn[TPFPC](Cl)	Sn	2.039	2.052	0.594	Cl	–	2.330	–	domed		GIYKIJ
94	51	Sb[TPFPC](F_2)	Sb	1.973	1.979	0.013	F	F	1.932	1.940	planar		YEBTEF
95	75	Re[TCF_3C](O)	Re	2.021	1.992	0.701	O	–	1.662	–	slightly domed		NUHJOP
96	75	Re[TCF_3C](O)	Re	2.019	1.992	0.701	O	–	1.657	–	slightly domed		NUHJOP01
97	77	Ir[TPFPC]($NMe_3)_2$	Ir	1.975	1.954	0.006	$N(CH_3)_3$	$N(CH_3)_3$	2.185	2.186	planar		COHYII
98	77	Ir[Br_8TPFPC]($NMe_3)_2$	Ir	1.988	1.961	0.001	$N(CH_3)_3$	$N(CH_3)_3$	2.187	2.192	planar		COHYOO
99	77	Ir[TPFPC]($Py)_2$	Ir	1.978	1.950	0.001	Py	Py	2.05	2.07	planar		YUHQIC
100	77	Ir[TPFPC]($NH_3)_2$	Ir	1.973	1.955	0.000	NH_3	NH_3	2.084	2.064	flat	–	IBABUK
101	79	Au[Br_8TPFPC]	Au	1.970	1.937	0.006	–	–	–	–	flat	–	UCEXUX
102	83	Bi[TPFPC]	Bi	2.260	2.225	1.122	–	–	–	–	domed	–	UCUPUF

Explanatory notes:

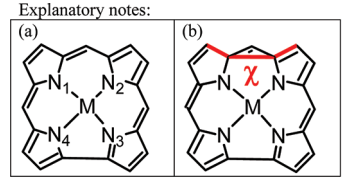

(c) Cambridge Structural Database (CSD), Version 5.33, Feb 2012 update.

TABLE 2. Abbreviations used in Table 1

abbreviation	explanation
BMePyPFPC	5,15-bis(*N*-methylpyridinium-4-yl)-10-(pentafluorophenyl)corrolato
Br_6TPC	5,10,15-triphenyl-2,3,8,12,17,18-hexabromocorrolato
Br_8(*p*OMeP)$_2$TC	2,3,7,8,12,13,17,18-octabromo-10-(4-methylphenyl)-5,15-bis(4-methoxyphenyl)corrolato
Br_8TNPC	2,3,7,8,12,13,17,18-octabromo-5,10,15-tris(4-nitrophenyl)corrolato
Br_8TPFPC	2,3,7,8,12,13,17,18-octabromo-5,10,15-tris(pentafluorophenyl)corrolato
BT-PFP-*p*BrP-C	5-(benzothiophen-2-yl)-10-(pentafluorophenyl)-15-(4-bromophenyl)corrolato
$(CF_3)_2$PFC	5,15-bis(trifluoromethyl)-10-(pentafluorophenyl)corrolato
$(CF_3)_8$T*p*FPC	2,3,7,8,12,13,17,18-(trifluoromethyl)-5,10,15-tris(*p*-fluorophenyl)corrolato
Dmes-Py*C	10-[4,6-bis(4-t-butylphenoxy)pyrimidin-5-yl]-5,15-dimesitylcorrolato
DNO_2-TPFPC	3,17-dinitro-5,10,15-tris(pentafluorophenyl)corrolato
DPFPThC	5,15-bis(pentafluororphenyl)-10-(3-thienyl)corrolato
DpivNP-TOMeP-C	10-(3,4,5-trimethoxyphenyl)-5,15-bis[2,6-bis(pivaloylamino)phenyl]corrolato
DP*p*OMePC	10-(*p*-methoxyphenyl)-5,15-diphenylcorrolato
Et_2Me_6C	8,12-diethyl-2,3,7,13,17,18-hexamethylcorrolato
$Et_4Me_2R_2$C	2,3,17,18-tetra-ethyl-8,12-bis[2-(methoxycarbonyl)ethyl]-7,13-dimethylcorrolato
Et_4Me_4C	2,3,7,8-tetraethyl-12,13,16,17-tetramethylcorrolato
$Et_4R_2Me_2$C	7,8,12,13-tetraethyl-2,18-bis[2-(methoxycarbonyl)ethyl]-3,17-dimethylcorrolato
Et_6Me_2C	2,3,8,12,17,18-hexaethyl-7,13-dimethylcorrolato
Et_8AcC	10-acetyl-2,3,7,8,12,13,17,18-octa-ethylcorrolato
Et_8Ph_2C	2,3,7,8,12,13,17,18-octaethyl-5,15-diphenylcorrolato
Et_8T_2C	2,3,7,8,12,13,17,18-octaethyl-5,15-bis(*p*-methylphenyl)corrolato
Et_8TPC	5,10,15-triphenyl-2,3,7,8,12,13,17,18-octamethylcorrolato
I_4TPFPC	2,3,17,18-tetraiodo-5,10,15-tris(pentafluorophenyl)corrolato
Me_4Ph_5C	7,8,12,13-tetramethyl-2,3,10,17,18-pentaphenylcorrolato
Me_8C	2,3,7,8,12,13,17,18-octamethylcorrolato
Me_8TPC	2,3,7,8,12,13,17,18-octamethyl-5,10,15-triphenylcorrolato
NO_2-TPFPC	3-nitro-5,10,15-tris(pentafluorophenyl)corrolato
OEC	2,3,7,8,12,13,17,18-octaethylcorrolato
(*p*CF_3P)$_2$*p*OMePC	10-(*p*-methoxyphenyl)-5,15-bis[*p*-(trifluoromethyl)phenyl]corrolato
Ps_2TPFPC	2,17-bis(piperidinylsulfonyl)-5,10,15-tris(pentafluorophenyl)corrolato
Ps_2TPFPC'	3,17-bis(piperidinylsulfonyl)-5,10,15-tris(pentafluorophenyl)corrolato
T2ThC	5,10,15-tris(2-thienyl)corrolato
T3ThC	5,10,15-tris(3-thienyl)corrolato
TPTBuC	5,10,15-triphenyl-2:3,7:8,12:13,17:18-tetrabutanocorrolato
TPTBzC	5,10,15-triphenyl-2:3,7:8,12:13,17:18-tetrabenzocorrolato
TC_3F_7C	5,10,15-tris(heptafluoropropyl)corrolato
TCbPC	5,10,15-tris[4-(1,2-dicarba-*closo*-dodecaboran-1-yl)phenyl]corrolato
TCF_3C	5,10,15-tris(trifluoromethyl)corrolato
TDCPC	5,10,15-tris(2,6-dichlorophenyl)corrolato
TMePyC	5,10,15-tris(*N*-methyl-*o*-pyridylium)corrolato
TNO_2-$Et_4R_2Me_2$C'	5,10,15-trinitro-2,3,17,18-tetraethyl-8,12-bis(methoxycarbonylmethyl)-7,13-dimethylcorrolato
TNO_2-TPFPC	2,3,17-trinitro-5,10,15-tris(pentafluorophenyl)corrolato
TPC	5,10,15-triphenylcorrolato
TPFPC	5,10,15-tris(pentafluorophenyl)corrolato
TPFPC-CHO	5,10,15-tris(pentafluorophenyl)corrolato-3-carbaldehyde
TPFPC-COOH	5,10,15-tris(pentafluorophenyl)corrolato-3-carboxylic acid
TpOMePC	5,10,15-tris(*p*-methoxyphenyl)corrolato
TTC	5,10,15-tri(*p*-methylphenyl)corrolato
TMesC	5,10,15-trimesitylcorrolato
TNPC	5,10,15-tris(4-nitrophenyl)corrolato
(*o*-TolPh)(PFP)$_2$C	10-(4,1'-biphenyl-1-yl)-5,15-bis(pentafluorophenyl)corrolato

corroles, including $Co^{III}[(CF_3)_3Cor](PH_3)$, and for copper porphine. Figure 6c compares the ruffling and saddling potentials for unsubstituted cobalt and copper corrole complexes. Note that the potential for the ruffling dihedral ψ is much steeper than that for the saddling dihedral χ. The result is nicely consistent with the fact that although ruffled metallocorroles are essentially nonexistent, saddled ones do occur, albeit infrequently.

A final question to consider in this connection is whether the impossibility of ruffling is a trivial issue for metallocorroles. Given that ruffling involves pyramidalization of the bipyrrolic double bond, it is not surprising, one might argue, that it is highly unfavorable. Pyramidalization of the bipyrrolic double bond does occur for domed corroles; that, however, never translates to ruffling, that is, alternate *twisting* of the pyrrole groups about the metal−nitrogen bonds.

5. Saddling: The Unique Case of Copper Corroles

The structural chemistry of copper corroles is of particular interest to us and a key highlight of this Account. Our interest in this area began with the observation some

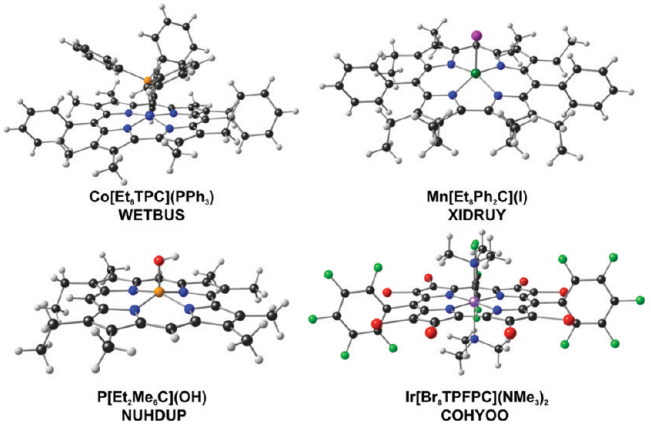

FIGURE 2. Examples of planar corroles.

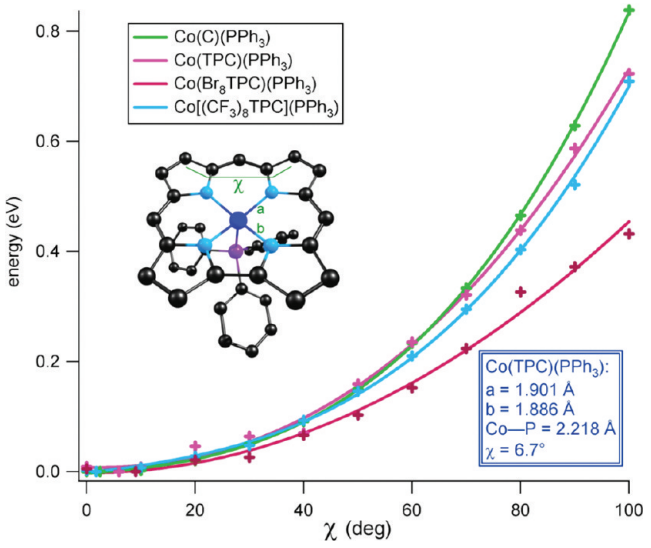

FIGURE 3. OLYP/STO-TZP saddling potentials for a set of four Co-PPh_3 corroles, involving progressively sterically hindered ligands: unsubstituted corrole (C), *meso*-triphenylcorrole (TPC), β-octabromo-*meso*-triphenylcorrole (Br_8TPC), and β-octakis(trifluoromethyl)-*meso*-triphenylcorrole [$(CF_3)_8$TPC].[21]

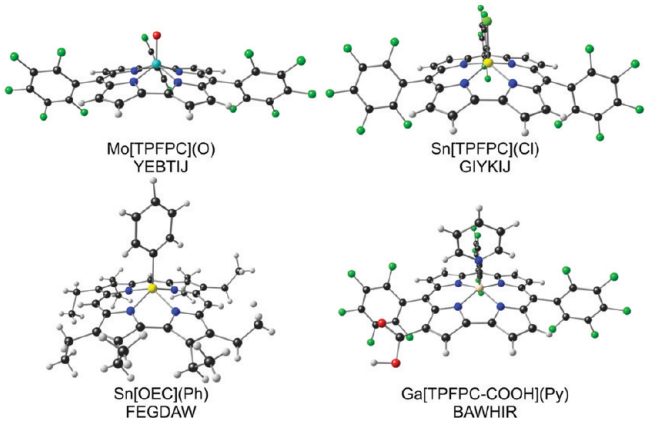

FIGURE 4. Examples of domed corroles.

three years ago that two sterically unhindered copper *meso*-triarylcorroles, Cu[DP*p*OMePC] (LUMDON) and Cu[($p$$CF_3$P)$_2$-*p*OMePC] (LUMDUT) (see Table 2 for ligand abbreviations), exhibited substantially saddled corrole rings with $\chi \approx 45°$ (Figure 7).[21] A survey of available crystal structures of copper corroles showed that they too were saddled, although for copper β-octaalkylcorroles (RINCAS,[22] QEVQAK[23]) the degree of saddling was more muted than that found for the triarylcorrole complexes examined by us. This was an intriguing observation, in view of the general rarity of saddled metallocorroles, prompting us to investigate the possibility of an electronic driving force behind the observed saddling. We therefore undertook a DFT study of copper complexes with four different corrole ligands: unsubstituted corrole, TPC, Br_8TPC, and $(CF_3)_8$TPC.

The saddling potentials of these four copper corroles are shown in Figure 8, and they capture much of the unique structural chemistry of these complexes.[21] First, a distinctly saddled minimum is indicated for even sterically unhindered copper corroles, including unsubstituted copper corrole and Cu[TPC]. Second, the degree of saddling can be significantly enhanced by introducing bulky β-substituents. Thus, a saddling dihedral of about 70° was predicted for Cu[Br_8TPC], whereas adjacent pyrrole rings in Cu[$(CF_3)_8$TPC] were predicted to be essentially orthogonal, rather a dramatic prediction for a class of porphyrinoids known to be exceptionally resistant to such distortions. Recall from Figure 3 that the analogous cobalt complexes were all predicted to be planar. Fortunately, crystal structures could be obtained for close analogues of all these copper complexes and to our considerable satisfaction they nicely confirmed the DFT predictions.

A crystal structure of the copper β-octabromo-*meso*-triarylcorrole Cu[Br_8(*p*OMeP)$_2$TC] (UKETAG)[24] revealed a saddling dihedral χ of 67.8°, in essentially perfect agreement with the OLYP/TZP value (67.0°). For Cu[$(CF_3)_8$T*p*FPC],[25] the observed χ of 84.5°, while dramatic, turned out to be somewhat lower than the OLYP value of 99.8° (Figure 9). As of today, these two complexes are the preeminent examples of strongly saddled corroles, which naturally raises a couple of questions. Why are such saddled structures so rare? Why are these two structures so strongly saddled?

The rarity of saddled metallocorroles and the fact that saddling seems to occur primarily for copper corroles strongly suggests the operation of a copper-specific metal–ligand orbital interaction.[26] Such an interaction is well-established for nickel and copper porphyrins, where saddling switches on a metal(d_{x2-y2})–porphyrin(a_{2u}-HOMO) interaction.

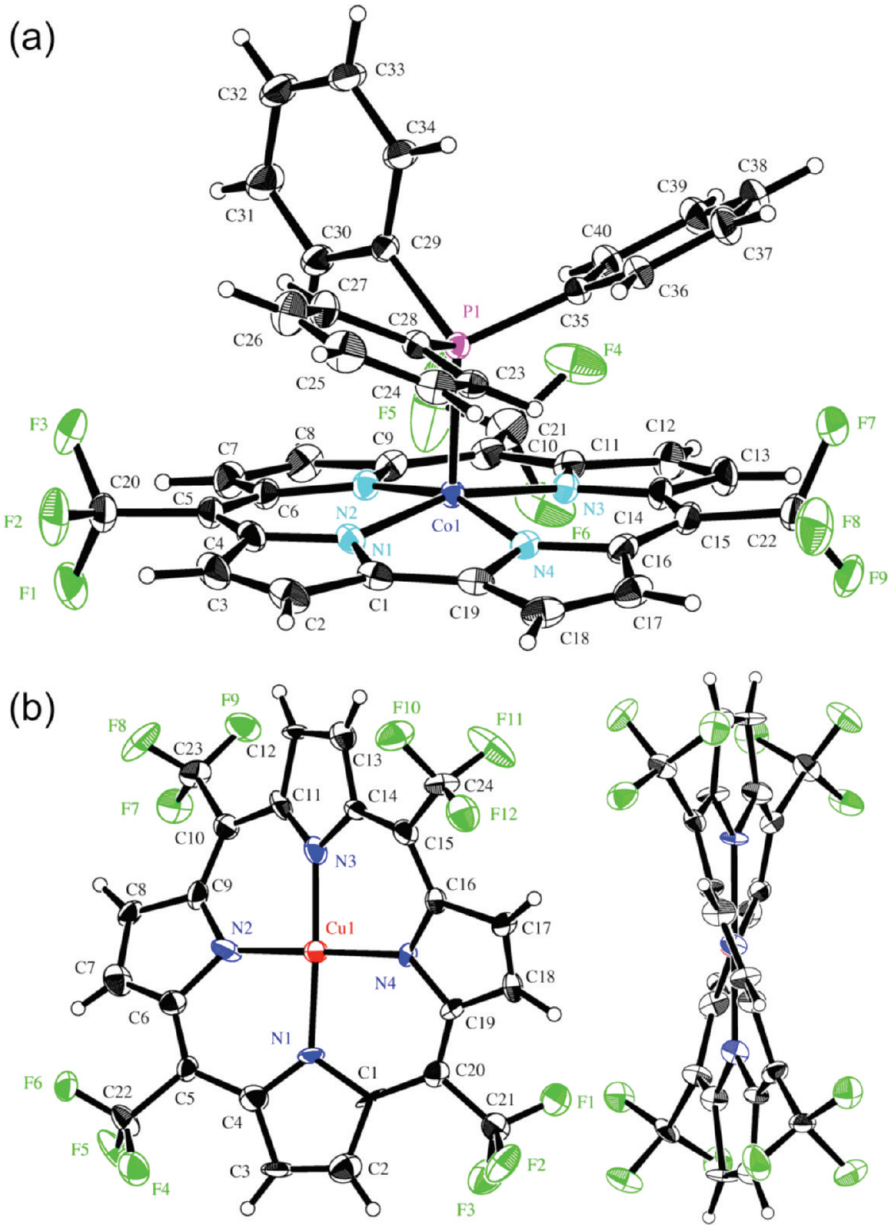

FIGURE 5. ORTEPs (20% thermal ellipsoids): (a) $Co^{III}[(CF_3)_3Cor](PPh_3)$ and (b) $Cu[(CF_3)_4Por]$ ("top" and "side" views).[12]

An exactly analogous scenario may be envisioned for metallocorroles, whose ring HOMOs closely resemble porphyrin HOMOs in shape. An examination of the HOMO of any copper corrole readily confirms this hypothesis, as illustrated in Figure 10 by the HOMO of Cu(TPC).[24] Saddling allows a good deal (about 50%) of the electron density from the β-symmetry (with reference to the C_2 point group) π-HOMO (the analogue of the porphyrin a_{2u}-HOMO) to flow into the space of the Cu d_{x2-y2} orbital. In other words, the metal center is not quite Cu(III), despite the short Cu−N distance, but has substantial Cu(II) character. Copper corroles are thus literally saddled with noninnocence!

Once the d_{x2-y2}−"a_{2u}" interaction is present as a driving force, sterically encumbering substituents can accentuate the saddling quite dramatically. In the absence of an electronic driving force, however, sterically encumbering substituents alone seem powerless to engender significant saddling.[27−29]

6. Gold Corroles

Although silver corroles have been known for some time, gold corroles have been reported only recently.[30] Like its iridium(III) analogues,[31] $Au[Br_8TPFPC]$ has turned out to be phosphorescent in the near-infrared.[32] In our laboratory, we have synthesized a series of Au(III)

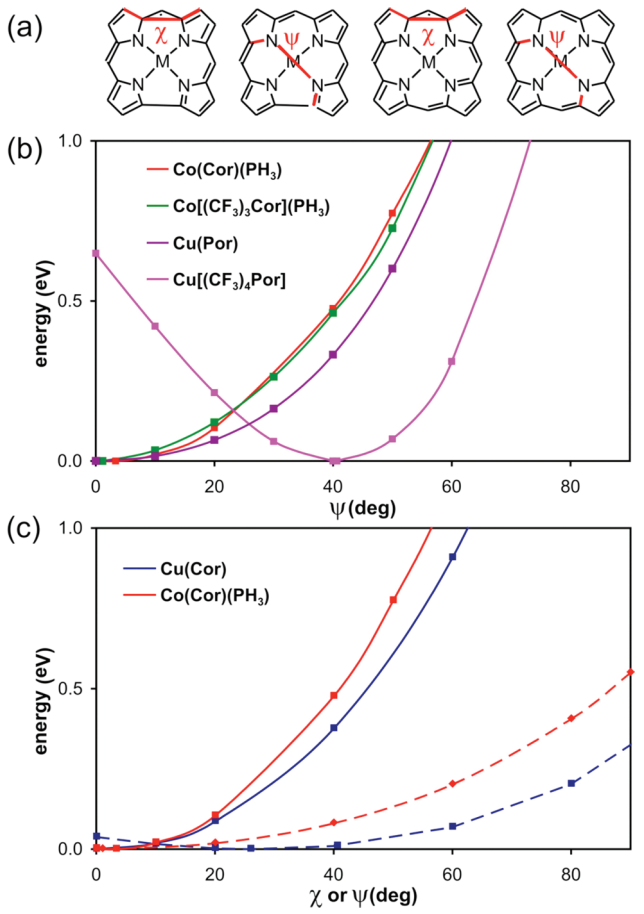

FIGURE 6. (a) Definition of ruffling (ψ) and saddling (χ) dihedrals; BP86-D/STO-TZP ruffling potentials for (b) Co and Cu porphyrins/corroles and (c) comparison of ruffling (solid lines) and saddling potentials (dotted lines).[12]

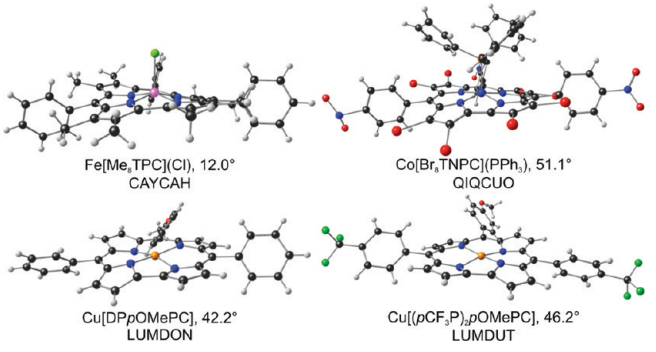

FIGURE 7. Examples of saddled corroles.

meso-tris(*p*-X-phenyl)corroles, Au[T*p*XPC], X = CF_3, F, H, CH_3, OCH_3, of which the *p*-F complex, Au[T*p*FPC], has lent itself to single-crystal X-ray structure determination.[33] The highly sterically hindered complex Au[$(CF_3)_8$T*p*FPC] could also be synthesized and crystallographically analyzed (Thomas, K. E.; Beavers, C. M.; Ghosh, A. Unpublished results).

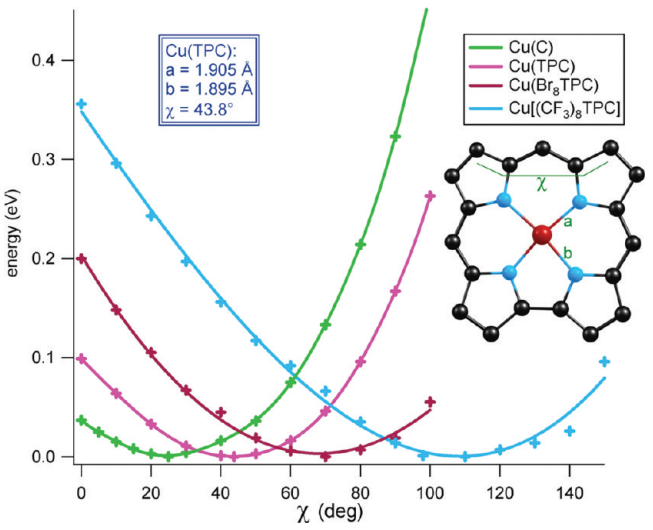

FIGURE 8. OLYP/TZP saddling potentials of four copper corroles, the ligands being unsubstituted corrole, TPC, Br_8TPC, and $(CF_3)_8$TPC.[21]

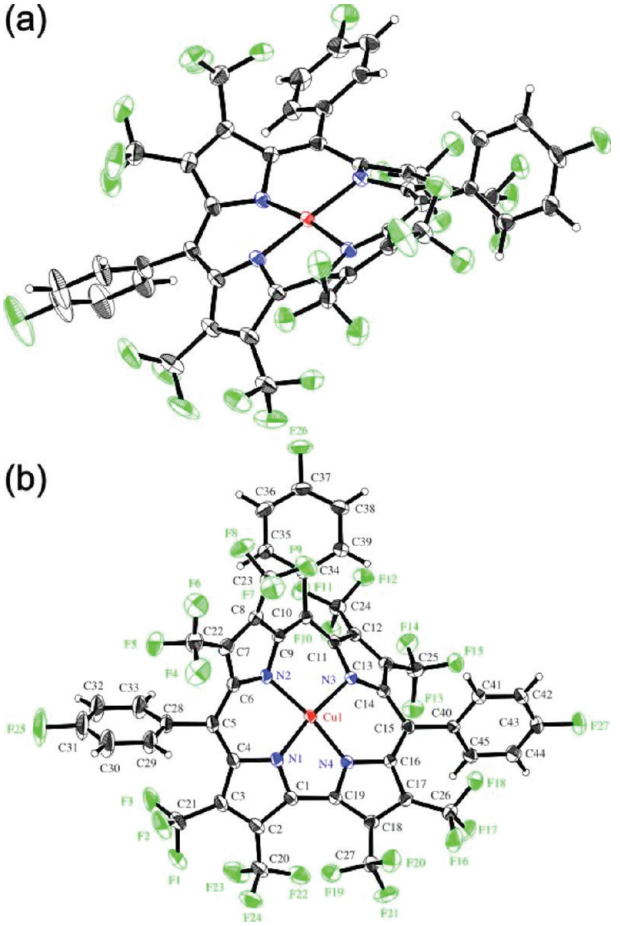

FIGURE 9. Two ORTEP views of Cu[$(CF_3)_8$T*p*FPC]. Distances (Å): Cu–N1 1.929(3), Cu–N2 1.922(4), Cu–N3 1.927(3), Cu–N4 1.914(4). Dihedrals (°): C3–C4–C6–C7 83.2, C8–C10–C11–C12 84.5, C13–C14–C16–C17 89.6, C2–C1–C19–C18 57.2.

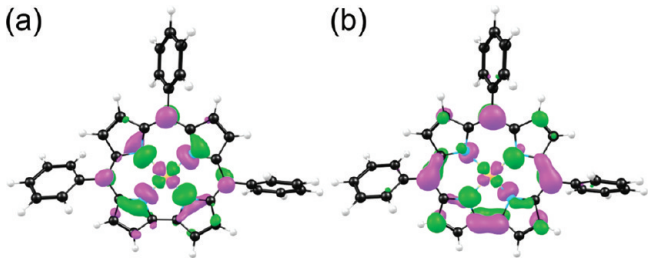

FIGURE 10. OLYP/TZP frontier orbitals of Cu(TPC): (a) LUMO and (b) HOMO.

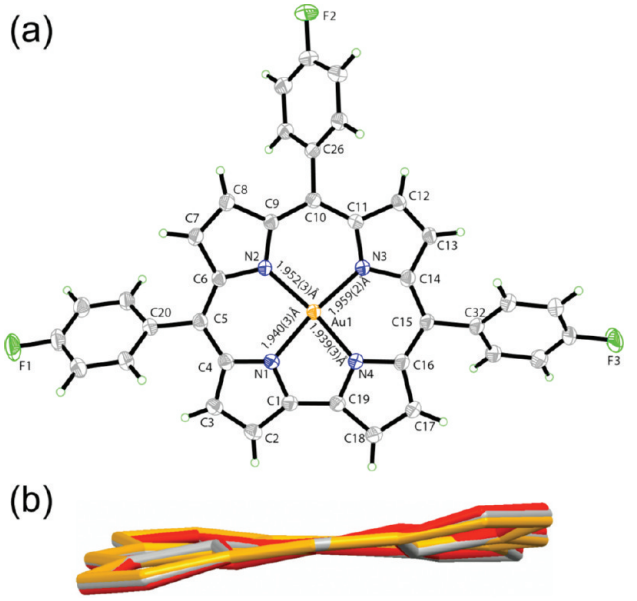

FIGURE 11. (a) Thermal ellipsoid (50%) diagram of Au[T(*p*-F)PC]. Disordered solvent was omitted for clarity. (b) Side-on view of Cu (red), Ag (gray), and Au (gold) corrole cores overlaid on one another.

Conformationally, the gold corroles have turned out to be very different from copper corroles.

Figure 11 depicts the crystal structure of Au[T*p*FPC] and overlays the corrole core with those of Cu and Ag analogues. Although the M−N distances differ only slightly between Cu (about 1.90 Å) and the heavier coinage metals (about 1.95 Å for both Ag and Au), the degree of saddling varies considerably. Thus, χ is only about 24.5° for Au[T*p*FPC], compared with a value of almost twice that (48.7°) for Cu[T*p*FPC]. The crystal structure of Au[$(CF_3)_8$TPC], shown in Figure 12, is even more remarkable; the corrole core is essentially perfectly planar. Between Au[$(CF_3)_8$TPC] and Cu[$(CF_3)_8$TPC], the saddling dihedral χ thus goes up by an astounding 85°!

7. Saddling as a Window Into Ligand Noninnocence

Even though our focus here is on structural chemistry, our main interest revolves around geometric structure,

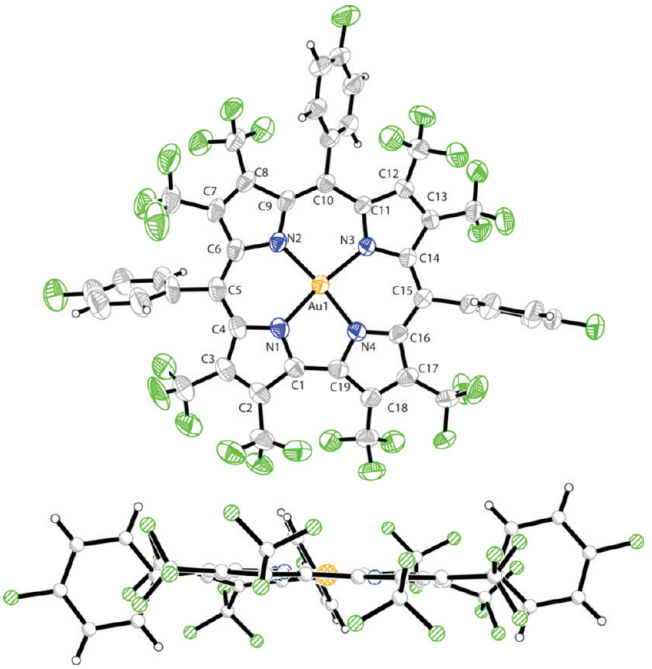

FIGURE 12. Crystal structure of Au[$(CF_3)_8$T(*p*-F)PC], with an essentially planar corrole core.

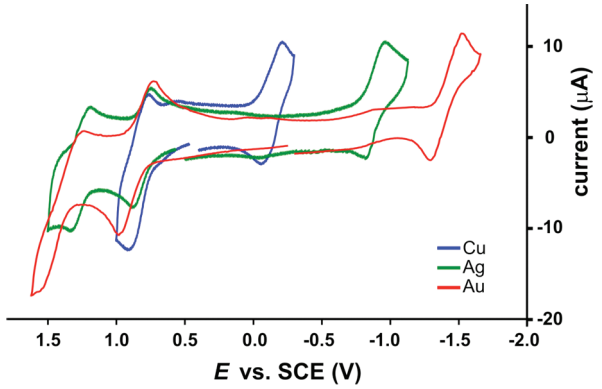

FIGURE 13. Cyclic voltammograms of M[T(*p*-F)PC], M = Cu, Ag, and Au, in CH_2Cl_2. See the Supporting Information for experimental details.

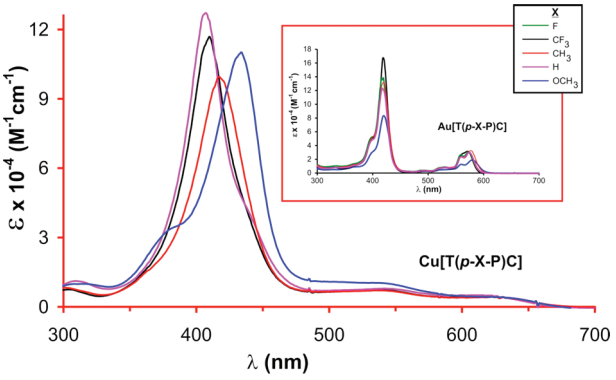

FIGURE 14. Electronic absorption spectra of Cu[T(*p*-X-P)C] in CH_2Cl_2. Inset: spectra of Au[T(*p*-X-P)C].

particularly saddling, as a window into electronic structure and the question of corrole noninnocence. We will illustrate this point through a consideration of the coinage metal corroles. Figure 13 presents the cyclic voltammograms of of M[T*p*FPC], M = Cu, Ag, and Au. The most striking aspect of these is that whereas the first oxidation potentials vary little across the coinage metal triad, the reduction potentials vary dramatically, becoming increasingly negative down the triad. Stated differently, the electrochemical "HOMO−LUMO gaps" (defined as the algebraic difference between the first oxidation and reduction potentials) widen dramatically down the triad, reflecting the increasingly higher energy of the valence d_{x2-y2} orbital. The high energy of this orbital for the heavier coinage metals, particularly Au, implies that there is little imperative for a metal(d_{x2-y2})−corrole("a_{2u}") interaction, explaining the relative lack of saddling for gold corroles.[32] The high energy of the d_{x2-y2} orbital also explains the lack of substituent effects on the Soret bands of Au[T*p*XPC], as a function of the *para* substituents X, as shown in Figure 14; by contrast, note the strong shifts in the Soret bands for Cu[T*p*XPC].

8. Conclusions and Perspectives

X-ray structure determinations, supplemented by quantum chemical calculations, have uncovered a number of trends in the structural chemistry of metallocorroles, which may be summarized as follows:

(a) Compared with metalloporphyrins, metallocorroles are much more resistant to nonplanar distortions.
(b) Of the various possible nonplanar distortions, only doming can be said to be moderately common; it is most commonly observed for five-coordinate metallocorroles.
(c) Ruffling, by contrast, is essentially a forbidden distortion mode for metallocorroles.
(d) Saddling is uncommon, but copper corroles, even sterically unhindered ones, are uniquely saddled as a result of an effective d_{x2-y2}−"a_{2u}" orbital interaction. This saddling can be dramatically accentuated by steric crowding on the corrole periphery.
(e) The high energy of the valence d_{x2-y2} orbital of Ag and Au is less conducive to saddling, relative to the copper case. Gold corroles, even sterically hindered ones, are thus relatively planar.

With these fundamentals in place, one might envision significantly more ambitious structural studies involving metallocorroles, involving supramolecular entities such as liquid crystals and metal−organic frameworks. In contrast to nonpolar D_{4h} metalloporphyrins, metallocorroles have polar point group symmetry, C_{2v} or one of its subgroups, and corrole-based supramolecular constructs are therefore expected to differ from porphyrin-based ones with respect to their symmetry properties. In our laboratory, we are particularly interested in exploiting the chirality of copper corroles and in developing novel oriented materials, such as chiral liquid crystals, based on copper corroles. These remain exciting goals for the future.

This work was supported largely by the Research Council of Norway. J.C. acknowledges the National Research Fund of the Republic of South Africa, while C.M.B. acknowledges the Advanced Light Source at Lawrence Berkeley National Laboratory. Other collaborators who have contributed to our research on metallocorroles include, among others, Dr. Ingar H. Wasbotten, Dr. Erik Steene, Dr. Emmanuel Gonzalez, Dr. Adam Chamberlin, Dr. Bruno Cardey, Prof. Lars-Kristian Hansen, Can Capar, Hans-Kristian Norheim, Simon Larsen, and Steffen Berg.

BIOGRAPHICAL INFORMATION

Kolle E. Thomas was born in Buea, Cameroon, in 1977. After receiving a B.Sc. in Chemistry from the University of Buea, he obtained his M.Sc. and subsequently a Ph.D. in chemistry from the University of Tromsø, Norway. Currently a postdoc with Prof. Abhik Ghosh, he is pursuing his interest in fluorinated porphyrins, corroles, and related ligands and their complexes.

Abraham Alemayehu was born in Shambu, Ethiopia. He received his B.Sc. in Chemistry from the University of Addis Ababa in 2000 and his M.Sc. and Ph.D. degrees from the University of Tromsø in 2005 and 2009, respectively. Alemayehu's research interests center around materials applications of porphyrins and related molecules.

Jeanet Conradie was born in Bloemfontein, South Africa, in 1956. She obtained a Master's degree in Physics from the University of Pretoria, South Africa. She received her Ph.D. in Chemistry working on rhodium and iridium complexes from the University of the Free State, South Africa, where she is now an Associate Professor of Chemistry. Her research interests involve novel transition metal complexes and intermediates, which she studies with both experimental and computational methods.

Christine Beavers was born in Oakland, California, USA. She is an Advanced Light Source postdoctoral fellow at Lawrence Berkeley National Laboratory. She obtained her B.Sc. and Ph.D. from the University of California, Davis. Her research interests focus on the structural characterization of complex chemical systems using crystallography. She is primarily concerned with exploiting the higher intensity of synchrotron radiation to push the boundaries of conventional crystallography.

Abhik Ghosh is a Professor of Chemistry at the University of Tromsø, Norway, where he has worked for the last 15 years. A native of West Bengal, India, he obtained his Ph.D. in 1992 from

the University of Minnesota, working with Professors Paul G. Gassman and Jan Almlöf. Between 1997 and 2004, he was also a Senior Fellow at the San Diego Supercomputer Center; subsequently (2004−2011), he has been an Outstanding Younger Researcher grantee of the Research Council of Norway. In recent years, he has spent several stints as a Visiting Professor at The University of Auckland, New Zealand. His research interests are at the intersection of bioinorganic, materials, and computational chemistry, and he has published approximately 150 papers in these areas. He serves or has served on the editorial advisory boards of the *Journal of Biological Inorganic Chemistry*, *Journal of Inorganic Biochemistry*, and *Journal of Porphyrins and Phthalocyanines*. He has edited two books, *The Smallest Biomolecules: Diatomics and Their Interactions with Heme Proteins* (Elsevier, 2008) and *Letters to a Young Chemist* (Wiley, 2011), the latter a popular book on chemistry research as a potential career option for high school and college students. One of his abiding passions is chemical education, where he attempts to develop "friendlier" approaches to teaching difficult theoretical and mechanistic concepts to younger undergraduates (see e.g., Berg, S.; Ghosh, A. *J. Chem. Educ.* **2011**, *88*, 1663−1666).

FOOTNOTES

*To whom correspondence should be addressed. E-mail: abhik@chem.uit.no.
The authors declare no competing financial interest.

REFERENCES

1 Falk, J. E. *Porphyrins and Metalloporphyrins*; Smith, K. M., Ed.; Elsevier: Amsterdam, 1975; pp 1−934.

2 Kadish, K. M.; Smith, K. M.; Guilard, R. *Handbook of Porphyrin Science, With Applications to Chemistry, Physics, Materials Science, Engineering, Biology and Medicine*; World Scientific: Singapore; Vols 1−10 (2010), Vols 11−15 (2011).

3 (a) Park, J. K.; Yoon, Z. S.; Yoon, M.-C.; Kim, K. S.; Mori, S.; Shin, J.-Y.; Osuka, A.; Kim, D. Solvent- and Temperature-Dependent Conformational Changes between Hückel Antiaromatic and Möbius Aromatic Species in meso-Trifluoromethyl Substituted [28]Hexaphyrins. *J. Am. Chem. Soc.* **2008**, *130*, 1824–1825. (b) Pacholska-Dudziak, E.; Skonieczny, J.; Pawlicki, M.; Szterenberg, L.; Ciunik, Z.; Latos-Grazynski, L. Palladium Vacataporphyrin Reveals Conformational Rearrangements Involving Hückel and Möbius Macrocyclic Topologies. *J. Am. Chem. Soc.* **2008**, *130*, 6182–6195.

4 Aviv-Harel, I.; Gross, Z. Aura of Corroles. *Chem.—Eur. J.* **2009**, *15*, 8382–8394.

5 (a) Gross, Z.; Galili, N.; Saltsman, I. The First Direct Synthesis of Corroles from Pyrrole. *Angew. Chem., Int. Ed.* **1999**, *38*, 1427–1429. (b) Paolesse, R.; Mini, S.; Sagone, F.; Boschi, T.; Jaquinod, L.; Nurco, D. J.; Smith, K. M. 5,10,15-Triphenylcorrole: a product from a modified Rothemund reaction. *Chem. Commun.* **1999**, 1307–1308. (c) Koszarna, B.; Gryko, D. T. Efficient Synthesis of meso-Substituted Corroles in a H_2O-MeOH Mixture. *J. Org. Chem.* **2006**, *71*, 3707–3717.

6 (a) Ghosh, A. A Perspective of Pyrrole-Aldehyde Condensations as Versatile Self-Assembly Processes. *Angew. Chem., Int. Ed.* **2004**, *43*, 1918–1931. (b) Gryko, D. T. Recent Advances in the Synthesis of Meso-Substituted Corroles and Core-Modified Corroles. *Eur. J. Inorg. Chem.* **2002**, 1735–1743.

7 Gouterman, M.; Wagniére, G. H.; Snyder, L. C. Spectra of Porphyrins. Part II. Four-Orbital Model. *J. Mol. Spectrosc.* **1963**, *11*, 108–115.

8 Ghosh, A.; Wondimagegn, T.; Parusel, A. B. J. Electronic Structure of Gallium, Copper, and Nickel Complexes of Corrole. High-Valent Transition Metal Centers Versus Noninnocent Ligands. *J. Am. Chem. Soc.* **2000**, *122*, 5100–5104.

9 (a) For a review, see: Walker, F. A.; Licoccia, S.; Paolesse, R. *J. Inorg. Biochem.* **2006**, *100*, 810–837. (b) For a high-level ab initio CASPT2 study, see: Roos, B. O.; Veryazov, V.; Conradie, J.; Taylor, P. R.; Ghosh, A. *J. Phys. Chem.* **2008**, *112*, 14099–14102.

10 Paolesse, R.; Licoccia, S.; Bandoli, G.; Dolmella, A.; Boschi, T. First Direct Synthesis of a Corrole Ring From a Monopyrrolic Precursor. Crystal and Molecular Structure of (Triphenylphosphine)(5,10,15-triphenyl-2,3,7,8,12,13,17,18-octamethylcorrolato)cobalt-(III)-Dichloromethane. *Inorg. Chem.* **1994**, *33*, 1171–1176.

11 Palmer, J. H.; Day, M. W.; Wilson, A. D.; Henling, L. M.; Gross, Z.; Gray, H. B. Iridium Corroles. *J. Am. Chem. Soc.* **2008**, *130*, 7786–7787.

12 Thomas, K. E.; Conradie, J.; Hansen, L. K.; Ghosh, A. Corroles Cannot Ruffle. *Inorg. Chem.* **2011**, *50*, 3247–3251.

13 (a) Luobeznova, I.; Raizman, M.; Goldberg, I.; Gross, Z. Synthesis and Full Characterization of Molybdenum and Antimony Corroles and Utilization of the Latter Complexes as Very Efficient Catalysts for Highly Selective Aerobic Oxygenation Reactions. *Inorg. Chem.* **2006**, *45*, 386–394. (b) Wagnert, L.; Berg, A.; Stavitski, E.; Berthold, T.; Kothe, G.; Goldberg, I.; Mahammed, A.; Simkhovich, L.; Gross, Z.; Levanon, H. Exploring the photoexcited triplet states of aluminum and tin corroles by time-resolved Q-band EPR. *Appl. Magn. Reson.* **2006**, *30*, 591–604. (c) Kadish, K. M.; Will, Adamian S.; V., A.; Walther, B.; Erben, C.; Ou, Z.; Guo, N.; Vogel, E. Synthesis and Electrochemistry of Tin(IV) Octaethylcorroles, (OEC)Sn(C_6H_5) and (OEC)SnCl. *Inorg. Chem.* **1998**, *37*, 4573–4577. (d) Saltsman, I.; Goldberg, I.; Gross, Z. One-step conversions of a simple corrole into chiral and amphiphilic derivatives. *Tetrahedron Lett.* **2003**, *44*, 5669–5673. (e) Reith, L. M.; Stiftinger, M.; Monkowius, U.; Knör, G.; Schoeflberger, W. *Inorg. Chem.* **2011**, *50*, 6788–6797.

14 (a) Yamamoto, Y.; Nadano, R.; Itagaki, M.; Akiba, K. Synthesis and Structure of Phosphorus(V) Octaethylporphyrins That Contain σ-Bonded Element-Carbon Bond: Characterization of a Porphyrin Bearing an R-P:O Bond and Relation of the Ruffling of the Porphyrin Core with the Electronegativity of the Axial Ligands. *J. Am. Chem. Soc.* **1995**, *117*, 8287–8288. (b) Akiba, K.; Nadano, R.; Satoh, W.; Yamamoto, Y.; Nagase, S.; Ou, Z.; Tan, X.; Kadish, K. M. Synthesis, Structure, Electrochemistry, and Spectroelectrochemistry of Hypervalent Phosphorus(V) Octaethylporphyrins and Theoretical Analysis of the Nature of the PO Bond in P(OEP)(CH_2CH_3)(O). *Inorg. Chem.* **2001**, *40*, 5553–5567.

15 Paolesse, R.; Boschi, T.; Licoccia, S.; Khoury, R. G.; Smith, K. M. Phosphorus complex of corrole. *Chem. Commun.* **1998**, 1119–1120.

16 Sakamoto, R.; Saito, S.; Shimizu, S.; Inokuma, Y.; Aratani, N.; Osuka, A. meso-Trifluoromethyl-substituted Subporphyrin from Ring-splitting Reaction of meso-Trifluoromethyl-substituted [32]Heptaphyrin(1.1.1.1.1.1.1). *Chem. Lett.* **2010**, *39*, 439–441.

17 Tse, M. K.; Zhang, Z.; Mak, T. C. W.; Chan, K. S. Synthesis of an oxorhenium(V) corrolate from porphyrin with detrifluoromethylation and ring contraction. *Chem. Commun.* **1998**, 1199–1200.

18 Simkhovich, L.; Goldberg, I.; Gross, Z. First syntheses and X-ray structures of a meso-alkyl-substituted corrole and its Ga(III) complex. *J. Inorg. Biochem.* **2000**, *80*, 235–238.

19 Goll, J. G.; Moore, K. T.; Ghosh, A.; Therien, M. J. Synthesis, Structure, Electronic Spectroscopy, Photophysics, Electrochemistry, and X-ray Photoelectron Spectroscopy of Highly-Electron-Deficient [5,10,15,20-Tetrakis(perfluoroalkyl)porphinato]zinc(II) Complexes and Their Free Base Derivatives. *J. Am. Chem. Soc.* **1996**, *118*, 8344–8354.

20 Kadish, K. M.; Lin, M.; Van Caemelbecke, E.; De Stefano, G.; Medforth, C. J.; Nurco, D. J.; Nelson, N. Y.; Krattinger, B.; Muzzi, C. M.; Jaquinod, L.; Xu, Y.; Shyr, D. C.; Smith, K. M.; Shelnutt, J. A. Influence of Electronic and Structural Effects on the Oxidative Behavior of Nickel Porphyrins. *Inorg. Chem.* **2002**, *41*, 6673–6687.

21 Alemayehu, A. B.; Gonzalez, E.; Hansen, L. K.; Ghosh, A. Copper Corroles Are Inherently Saddled. *Inorg. Chem.* **2009**, *48*, 7794–7799.

22 Will, S.; Lex, J.; Vogel, E.; Schmickler, H.; Gisselbrecht, J. P.; Haubtmann, C.; Bernard, M.; Gross, M. Nickel and Copper Corroles: Well-Known Complexes in a New Light. *Angew. Chem., Int. Ed.* **1997**, *36*, 357–361.

23 Bröring, M.; Bregier, F.; Tejero, E. C.; Hell, C.; Holthausen, M. C. Revisiting the Electronic Ground State of Copper Corroles. *Angew. Chem., Int. Ed.* **2007**, *46*, 445–448.

24 Alemayehu, A. B.; Gonzalez, E.; Ghosh, A. Nonplanar, Noninnocent, and Chiral: A Strongly Saddled Metallocorrole. *Inorg. Chem.* **2010**, *49*, 7608–7610.

25 Thomas, K. E.; Conradie, J.; Hansen, L. K.; Ghosh, A. A Metallocorrole with Orthogonal Pyrrole Rings. *Eur. J. Inorg. Chem.* **2011**, 1865–1870.

26 Alemayehu, A. B.; Conradie, J.; Ghosh, A. A First TDDFT Study of Metallocorrole Electronic Spectra: Copper meso-Triarylcorroles Exhibit Hyper Spectra. *Eur. J. Inorg. Chem.* **2011**, *12*, 1857–1864.

27 We are aware of at least two noncoinange metal corroles that are significantly saddled; both are undecasubstituted: Co[Br_8TNPC](PPh_3) (QIQCUO)[27] and Fe[Me_8TPC](Cl) (CAYCAH).[28] Revisiting the saddling potentials shown in Figure 3 with dispersion-corrected DFT suggests that, for sterically hindered, undecasubstituted metallocorroles, saddling might not be quite as prohibitive as implied by Figure 3, even though planar structures are still the norm.

28 Paolesse, R.; Nardis, S.; Sagone, F.; Khoury, R. G. Synthesis and Functionalization of Meso-Aryl-Substituted Corroles. *J. Org. Chem.* **2001**, *66*, 550–556.

29 Nardis, S.; Paolesse, R.; Licoccia, S.; Fronczek, F. R.; Vicente, M. G. H.; Shokhireva, T. K.; Cai, S.; Walker, F. A. NMR and Structural Investigations of A Nonplanar Iron Corrolate: Modified Patterns of Spin Delocalization and Coupling in A Slightly Saddled Chloroiron(III) Corrolate Radical. *Inorg. Chem.* **2005**, *44*, 7030–7046.

30 Alemayehu, A. B.; Ghosh, A. Gold Corroles. *J. Porphyrins Phthalocyanines* **2011**, *15*, 106–110.

31 Palmer, J. H.; Durrell, A. C.; Gross, Z.; Winkler, J. R.; Gray, H. B. Near-IR Phosphorescence of Iridium(III) Corroles at Ambient Temperature. *J. Am. Chem. Soc.* **2010**, *132*, 9230–9231.

32 Rabinovitch, E.; Goldberg, I.; Gross, Z. Gold(I) and Gold(III) Corroles. *Chem.—Eur. J.* **2011**, *17*, 12294–12301.

33 Thomas, K. E.; Alemayehu, A. B.; Conradie, J.; Beavers, C.; Ghosh, A. Synthesis and Molecular Structure of Gold Triarylcorroles. *Inorg. Chem.* **2011**, *50*, 12844–12851.